– Supplementary Information –

Nanomechanical Torsional Resonators for Frequency-Shift Infrared Thermal Sensing

X. C. Zhang[1], E. B. Myers[1], J. E. Sader[1,2], M. L. Roukes[1*]

[1]*Kavli Nanoscience Institute and Condensed Matter Physics, California Institute of Technology, Mail Code 149-33, Pasadena, CA 91125, USA*
[2]*Department of Mathematics and Statistics, The University of Melbourne, Victoria 3010, Australia*

1. Temperature Coefficient of Frequency (*TCF*) for the torsional and flexural modes of the paddle resonator

The *TCF* of the flexural mode possesses an additional thermal stress term which is absent for the torsional mode. The mode-dependent thermal sensitivities originate from the distinct roles that stress plays in the motion. Figure S1 illustrates how the tensile force ***T*** enters into the equation of motion of the flexural mode, but not into the torsional motion

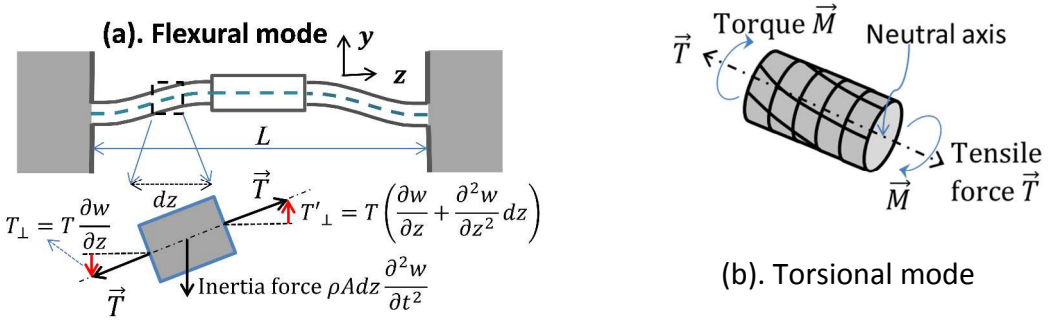

Fig. S1. (a), in the flexural mode, the tensile force *T* has a component along the direction of beam motion *z*, and thus contibutes to its resonant frequency and *TCF*, see text. In the equations, *w* is the displacement in the *y* direction. For the torsional mode (b), the tensile force *T* is along the direction of torsional axis, and generates no torque. Therefore, the tensile force dose not affect the torsional resonant frquency. This leads to an exceptionally linear torsional mode with a reduced *TCF*.

*E-mail: roukes@caltech.edu

1.1 The flexural mode resonant frequency and *TCF* of a stressed torsional resonator

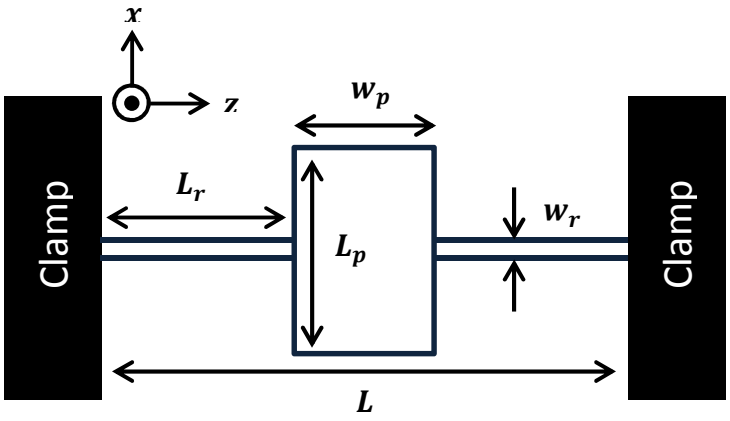

L_r = Torsion rod length
w_r = Torsion rod width
h = Device thickness

L_p = Paddle length
w_p = Paddle width
L = Device whole length

Fig. S2. A plane view diagram of the torsional device with the geometry labels. Origin of the coordinate system is at the center of the left hand clamped end.

We derive the resonant frequency of a doubly clamped torsional resonator with a built-in stress T. A schematic of the torsional device is given in Fig. S2. The coordinate system employed in this manuscript is also defined, with the origin set at the left end of the beam. The governing equation for the beam deflection function w is

$$\frac{\partial^2}{\partial \xi^2}\left(\frac{EI}{L^4}\frac{\partial^2 w}{\partial \xi^2}\right) - \frac{T}{L^2}\frac{\partial^2 w}{\partial \xi^2} + \mu\frac{\partial^2 w}{\partial t^2} = 0 \,, \tag{S1}$$

where $\xi = z/L$ is the reduced distance along the beam length L, I is the areal moment of inertia, E is the Young's modulus, t is time, and $\mu = \rho A$ is the mass per unit length.

Since the width of the paddle L_p greatly exceeds that in the arm w_r, we consider the paddle to be rigid relative to the narrow arms, and assume the inertia of the rods is negligible. We therefore ignore the inertial term in Eq. S1, and include the inertia only through the shearing force at the contact point between the rods and the paddle. This gives the governing equations and boundary conditions:

$$\frac{EI}{L^4}\frac{\partial^4 w}{\partial \xi^4} - \frac{T}{L^2}\frac{\partial^2 w}{\partial \xi^2} = 0\,, \tag{S2}$$

with the usual clamped boundary conditions:

$$\left[w = \frac{\partial w}{\partial \xi}\right]_{\xi=0} = \left.\frac{\partial w}{\partial \xi}\right|_{\xi=\overline{L_r}} = 0\,. \tag{S3a}$$

Applying Newton's 2nd law at the paddle

$$\left.\frac{EI}{L^3}\frac{\partial^3 w}{\partial \xi^3}\right|_{\xi=\overline{L_r}} = \frac{1}{2} M_p \left.\frac{\partial^2 w}{\partial t^2}\right|_{\xi=\overline{L_r}}\,, \tag{S3b}$$

where $\overline{L_r} = L_r/L$, M_p is the mass of the paddle, and the factor of ½ in Eq. S3b accounts for the symmetry of the resonator , i.e. that there are two identical narrow torsion rods.

The displacement is expressed in terms of an explicit time dependence $\exp(-i\omega t)$:

$$w(\xi, t) = W(\xi)exp(-i\omega t). \tag{S4}$$

Substituting Eq. S4 into Eq. 2 and 3 gives

$$\frac{d^4 W}{d\xi^4} - \upsilon \frac{d^2 W}{d\xi^2} = 0\,, \tag{S5}$$

with boundary conditions

$$\left[W = \frac{dW}{d\xi}\right]_{\xi=0} = \left.\frac{dW}{\partial \xi}\right|_{\xi=\overline{L_r}} = 0\,, \tag{S6a}$$

$$\left.\frac{EI}{L^3}\frac{d^3 W}{d\xi^3}\right|_{\xi=\overline{L_r}} = \frac{1}{2} M_p \omega^2 W\Big|_{\xi=\overline{L_r}}\,, \tag{S6b}$$

where the normalized tension parameter υ is

$$\upsilon = \frac{TL^2}{EI} \tag{S7}$$

Note that the required resonant frequency ω only appears in the boundary condition S6b. This property allows for an explicit determination of ω by solving the system in Eqs. S5-7:

$$\omega^2 = \frac{24EI}{M_p L_r^3} f(\upsilon) \tag{S8}$$

where

$$f(\upsilon) = \frac{\overline{L_r^2}\upsilon}{12}\left\{1 - \frac{2}{\overline{L_r}\sqrt{\upsilon}}\tanh\left(\frac{\overline{L_r}\sqrt{\upsilon}}{2}\right)\right\}^{-1} \tag{S9}$$

We can remove the scaling with respect to the total beam length L. Eqs. S8-9 then become:

$$\omega^2 = \frac{24EI}{M_p L_r^3} g(\tau), \tag{S10}$$

where

$$g(\tau) = \frac{\tau}{12}\left\{1 - \frac{2}{\sqrt{\tau}}\tanh\left(\frac{\sqrt{\tau}}{2}\right)\right\}^{-1}, \tag{S11a}$$

$$\tau = \frac{TL_r^2}{EI}. \tag{S11b}$$

For a rectangular cross section resonator, $I = w_r h^3/12$, Eq. S10 then simplifies to

$$\omega^2 = \frac{2Ew_r h^3}{M_p L_r^3} g(\tau), \tag{S12}$$

Using $\tanh(x) = x - \frac{x^3}{3} + \frac{2}{15}x^5 - \frac{17}{315}x^7 + \cdots$, in the limit of small tension, Eq. S11a becomes

$$g(\tau) = 1 + \frac{\tau}{10} + O(\tau^2). \tag{S13}$$

Equation S12 and S13 show that the resonant frequency reduces to the result of Evoy et al.[1] at zero tension case, i.e., $\omega_0 = \sqrt{\frac{2Ew_r h^3}{M_p L_r^3}}$. Substituting Eq. S12 into S13 gives the resonant frequency for a low stressed device

$$\omega \approx \sqrt{\frac{2Ew_r h^3}{M_p L_r^3}\left(1 + \frac{\tau}{10}\right)} \approx \omega_0\left(1 + \frac{\tau}{20}\right). \tag{S14}$$

We can rewrite Eq. S11b as

$$\tau = \frac{12\sigma L_r^2}{Eh^2}, \tag{S15}$$

where $\sigma=T/A=(\sigma_i-\alpha E\Delta T)$ is the tensile stress of the beam, σ_i is the intrinsic stress resulting from the wafer growth process, $\alpha E\Delta T$ is the thermal stress term that accounts for the IR (or any other sources) heating induced beam softening effect, where $\alpha = \frac{1}{l}\frac{dl}{dT}$ is the linear thermal expansion coefficient. The 1st derivative of Eq. S15 with the temperature yields:

$$TCF|_{\text{flexural}} = \frac{1}{f_0}\frac{df}{dT} = \frac{\alpha+\beta}{2} - \frac{3}{5}\left(\frac{L_r}{h}\right)^2 .\alpha, \tag{S16}$$

where $\beta = \frac{1}{E}\frac{dE}{dT}$ is the thermal coefficient of Young's modulus.

1.2 *TCF* of the torsional mode

The intrinsic resonant frequency of the torsional motion is given by

$$f_0 = \frac{1}{2\pi}\sqrt{\frac{\kappa}{I}} \tag{S17}$$

where I is the moment of inertia of the resonator, κ is the torsional spring constant.

Moment of Inertia

The moment of inertia for the two torsion rods is

$$I_R = \frac{1}{6}m_R(w_r^2 + h^2), \tag{S18a}$$

where m_R is the mass, w_r is the width, and h is the thickness of the torsional rod.

The paddle's moment of inertia is:

$$I_p = \frac{1}{12}M_p L_p^2, \tag{S18b}$$

here m_p and L_p are the mass and length of the paddle, respectively. The total moment of inertia is:

$$I = I_R + I_p \approx I_p = \frac{1}{12} M_p L_p^2. \quad \text{(S19)}$$

The last approximation holds true if $L_p \gg w_r, h$, which is the case for our device.

Torsional spring constant

For macroscopic beams of rectangular cross sections, the torsional spring constant can be calculated by[2]

$$\kappa = 2KG_s/L_r, \quad \text{(S20)}$$

where G_s is the shear modulus of the rod, which is related to Young's modulus by the relation $G_s = \frac{E}{2(\upsilon_p+1)}$, υ_p is Poisson′s ratio. L_r is the length of each rod, K is the torsional moment of inertia. For a rectangular cross section with sides of length h and w_r, where $h>w_r$, the torsional moment is given by[2]

$$K = hw_r^3 \left[\frac{1}{3} - 0.21 \frac{w_r}{h}(1 - \frac{h^4}{12\mathrm{w}_r^4})\right] \text{ for } h \geq \mathrm{w}_r. \quad \text{(S21)}$$

Combing all above, the torsional resonant frequency is given by

$$f = \frac{1}{2\pi}\sqrt{\frac{k}{(I_R + I_P)}} \approx \frac{1}{2\pi}\sqrt{\frac{k}{I_P}} = \frac{1}{2\pi}\sqrt{\frac{24K}{M_p} G \frac{hw_r^3}{L_p^2 L_r}}. \quad \text{(S22)}$$

The first derivative with temperature of Eq. S22 yields

$$TCF|_{\text{torsion}} = \frac{\alpha + \beta}{2} \quad \text{(S23)}$$

2. NETD limited by temperature fluctuation noise process

The spectral density of the thermodynamically driven temperature fluctuations are[3]

$$S_T(\omega) = \frac{2}{\pi}\frac{4k_B T^2}{G}\frac{BW}{1 + \omega_m^2 \tau^2}, \quad \text{(S24)}$$

where BW is the measurement bandwidth. The temperature fluctuations can be converted into noise equivalent power by

$$\delta P_{TF} = G.S_T^{\frac{1}{2}}(\omega). \quad \text{(S25)}$$

The amount of power received by an IR detector δP_t can be related to the temperature difference δT of a target relative to its surroundings (assuming blackbody radiation) by the following formula[3]

$$\delta P_t = \frac{\eta A_d}{4F^2}\left(\frac{dP}{dT}\right)_{\lambda_1,\lambda_2}\delta T_t, \tag{S26}$$

where A_d is the detector area, F is the focal ratio of the optics, and $\left(\frac{dP}{dT}\right)_{\lambda_1,\lambda_2}$ is the slope of the function $P=f(T_t)$, where P is the power radiated by a blackbody target within the spectral band from λ_1 to λ_2. For the long wavelength infrared band from 8-14 μm, dP/dT = 2.62 W/m^2·K. The NETD limited by the temperature fluctuation can be determined by combing Eq. S25 and S26.

The calculated NETD limited by the temperature fluctuations versus thermal conductance is depicted by the blue curve in Fig. 1d. The adopted parameters in the calculation are: ω_m=10 Hz, BW=1 Hz, $\eta = 0.3$, F=0.5. The device has the same geometry as shown in Fig. 1b.

3. Device fabrication process

The pattern of the torsional device is defined by the electron beam lithography, followed by the gold film, Strontium Fluoride (SrF_2) film deposition, and lift-off process. The device is released in a Sulfur Hexafluoride (SF6) based inductively coupled plasma (ICP) dry etching step with SrF_2 as the etching mask. The obtained narrowest supporting rod is 50 nm. The ICP etching offers a high lateral etching ratio between Si and SiN over 100:1, a Si lateral etching rate ~ 1 μm/min, a uniform and smooth etched surface over a whole 4 inch wafer.

4. Modeling of the optical interference technique

We develop a simple interference model to account for the optical transduction nonlinear effect. Assuming the interference cavity, commonly formed by the device top surface and the

substrate with a separation of d, the laser electric fields reflected from the cavity's top and bottom surfaces are:

$$E_1(\boldsymbol{r},t) = A_1(\boldsymbol{r})e^{i[\emptyset_0(\boldsymbol{r})-\omega' t]}, \quad (S27)$$

$$E_2(\boldsymbol{r},t) = A_2(\boldsymbol{r})e^{i[\emptyset_0(\boldsymbol{r})+2kd-\omega' t]}, \quad (S28)$$

where $\phi_0(\boldsymbol{r})$ is the initial phase, k is the wave vector, and ω' is the angular frequency of the laser light. The summed field is $U(r,t) = E_1(\boldsymbol{r},t) + E_2(\boldsymbol{r},t)$, and the interference intensity $I(\boldsymbol{r})$ is given by

$$I(\boldsymbol{r},d) = \int U(\boldsymbol{r},t)U^*(\boldsymbol{r},t)dt = A_1^2(\boldsymbol{r}) + A_2^2(\boldsymbol{r}) + 2A_1(\boldsymbol{r})A_2(\boldsymbol{r})\cos(2kd) \quad (S29)$$

This sets the background DC intensity that the photodetector measures. When the device vibrates at an amplitude of $\pm x$, the interference intensity, $I(\boldsymbol{r})$, becomes modulated. The modulation depth in $I(\boldsymbol{r})$, ΔI, is recorded by the photodetector as the measure of the device resonant amplitude, i.e. the optical displacement signal:

$$\Delta I = |I(\boldsymbol{r},d+x) - I(\boldsymbol{r},d-x)| = 4A_1(\boldsymbol{r})A_2(\boldsymbol{r})\sin(2kd)\sin(2kx) = A\sin(2kx) \quad (S30)$$

5. Optical nonlinearity caused resonance peak splitting versus actuation level

We quantify the resonance splitting caused by the optical nonlinearity as a function of the actuation level based on a driven damped resonator model. The amplitude of a driven damped resonator is given by

$$a(\omega) = \frac{F^2(\omega)}{M_{eff}^2[(\omega^2-\omega_0^2)^2 + \omega^2\omega_0^2/Q^2]} \quad (S31)$$

At the critical drive, the device reaches its maximum optical response at an amplitude $x_c = \lambda/8$ according to Eq. S30. The two frequencies corresponding to this amplitude according to above equation are

$$\omega_{\pm} = \omega_0 \sqrt{\left(1 - \frac{1}{2Q^2}\right) \pm \frac{1}{Q}\sqrt{\left(\frac{x}{x_c}\right)^2 - 1}} \approx \omega_0 \pm \frac{\omega_0}{2Q}\sqrt{\left(\frac{x}{x_c}\right)^2 - 1} \qquad (S32)$$

Finally the splitting is

$$\Delta\omega = \frac{\omega_0}{Q}\sqrt{\left(\frac{x}{x_c}\right)^2 - 1} = \frac{\omega_0}{Q}\sqrt{\left(\frac{V}{V_c}\right)^2 - 1}\ , \qquad (S33)$$

V is the applied RF voltage on the piezo-ceramic disk, V_c is the voltage corresponding to $a_c = \lambda/8$. The piezo-ceramic disk acts as a linear actuator in the whole power range of our experiments.

6. Dynamic range (DR) of the torsional mode

Since the torsional mode is inherently linear, its DR range should be limited by its elastic limit, *i.e.* the yield strength of the torsional rod τ_{ys}. The experimental elastic limit of SiN is about 12 GPa.[4] The maximum shear stress occurs at the outer surface of the torsional rod can be expressed as [2]

$$\tau_{max} = \frac{T_{max}}{\pi r^3}, \qquad \text{(for circular rod with a radius r)} \qquad (S34a)$$

$$\tau_{max} = \frac{3T_{max}}{2hw^2}\beta\left(\frac{w}{h}\right) \quad \text{(for rectangular rod with cross section length } h > w\text{)}, \qquad \text{(S34b)}$$

Where $\beta'\left(\frac{w_r}{h}\right) = 1 + 0.6095\frac{w}{h} + 0.8865(\frac{w}{h})^2 - 1.8023\left(\frac{w}{h}\right)^3 + 0.91(\frac{w}{h})^4$, T_{max} is the maximum torque applied to the torsional rod under the elastic limit, i.e., $\tau_{max} \leq \tau_{ys}$. The maximum displacement angle $\theta_{max} = T_{max}/\kappa$, where κ is the torsional constant expressed in Eq. S20, can be formulated as:

$$\theta_{max} = \frac{L}{r}\frac{\tau_{ys}}{G}, \text{(for circular rod)} \qquad (S35a)$$

$$\theta_{max} = \frac{1}{3\beta\left(\frac{w}{h}\right).\beta'\left(\frac{w}{h}\right)}.\frac{L}{w}.\frac{\tau_{ys}}{G}, \text{ (for rectangular rod),} \quad \text{(S35b)}$$

We simply consider the thermomechanical noise as the lower limit of the maximally-attainable DR. The spectral density of the angular displacement noise on resonance $S_\theta^{1/2} = \sqrt{4k_BT.Q/\omega_0\kappa}$ is

$$S_\theta^{1/2} = \left(\frac{64k_B^2T^2Q^2\rho}{3\pi^3G^3}.\frac{L_pL_r^3w_p^3}{r^{11}}\right)^{1/4}, \text{(for circular rod)} \quad (S36a)$$

$$S_\theta^{1/2} = \left(\frac{k_B^2T^2Q^2\rho}{\beta^3G^3}.\frac{L_pL_r^3w_p^3}{h^2w_r^9}\right)^{1/4}, \text{ (for rectangular rod)} \quad \text{(S36b)}$$

where L_p, L_r, w_p, w_r are the length and width of the torsional rod and paddle, respectively.

The DR of the torsional mode is defined as $\text{DR (dB)} = 20\log\left(\frac{\theta_{max}}{\sqrt{2S_\theta BW}}\right)$, BW=1Hz is the measurement bandwidth. It can be formulated as:

$$DR = 20\log\left[\frac{1}{2\sqrt{2}}.\tau_{ys}.\left(\frac{3\pi^3}{4k_B^2T^2Q^2\rho G}.\frac{\boldsymbol{r^7L_r}}{\boldsymbol{L_pw_p^3}}\right)^{1/4}\right], \text{(for circular rod)} \quad (S37a)$$

$$DR = 20\log\left[\frac{1}{3\sqrt{2}\beta'}.\tau_{ys}.\left(\frac{3\pi^3}{k_B^2T^2Q^2\beta\rho G}.\frac{\boldsymbol{h^2L_rw_r^5}}{\boldsymbol{L_pw_p^3}}\right)^{1/4}\right], \text{ (for rectangular rod)} \quad \text{(S37b)}$$

7. Allan deviation: its definition and measurement method

The Allan deviation (AD) is a time variance of the measured frequency of a source, each measurement averaged over a time interval τ_A. It is defined as $\sigma_A^2 = \frac{1}{2f_c^2}\frac{1}{N-1}\sum_{m=2}^{N}\left(\overline{f_m} - \overline{f_{m-1}}\right)^2$,[5] where $\overline{f_m}$ is the average frequency measured over the m_{th} time interval of length Δt=τ_A, and f_c is the nominal carrier frequency.

To measure AD, the device was driven at its resonant frequency f_0 by a CW signal, and the real time phase fluctuations were recorded in an open-loop configuration by a network analyzer. The measured phase can be converted to frequency by dividing the predetermined slope $2Q/f_0$ in the linear region of the phase-frequency resonance curve. The fastest sampling period in our measurements is limited to 100 ms by the data bus transfer speed.

REFERENCES

[1] Evoy S.; Carr D. W.; Sekaric L.; Olkhovets A.; Parpia J. M.; Craighead H. G. *J. Appl. Phys* 1999, 86, 6072-6077.

[2] Young W. C.; Budynas R. G.; Sadegh A. *Roark's Formulas for Stress and Strain*, 8th Ed., New York: McGraw-Hill, C2012.

[3] Krause P. W.; Skatrud D. D. "Uncooled Infrared Imaging Arrays and Systems", *Semicond. & Semimetals* 47, Academic press, 1997.

[4] Nathenson, D. I., "Experimental Investigation of High Velocity Impacts on Brittle Materials", PhD thesis, Case Western Reserve University, May 2006.

[5] Cleland A. N.; Roukes M. L. J. Appl. Phys. 2002, 92, 2758-2769.